



Preparation and *in vitro* properties of redox-responsive polymeric nanoparticles for paclitaxel delivery

Na Song^{a,1}, Wenming Liu^{a,1}, Qin Tu^a, Rui Liu^a, Yanrong Zhang^a, Jinyi Wang^{a,b,*}

^a Colleges of Science and Veterinary Medicine, Northwest A&F University, Yangling, Shaanxi 712100, PR China

^b Shaanxi Key Laboratory of Molecular Biology for Agriculture, Northwest A&F University, Yangling, Shaanxi 712100, PR China

ARTICLE INFO

Article history:

Received 29 April 2011

Accepted 7 June 2011

Available online 15 June 2011

Keywords:

Redox
Polymer
Nanoparticle
Paclitaxel
Delivery

ABSTRACT

Rice-like polymeric nanoparticles (NPs) composed of a new redox-responsive polymer, poly(ethylene glycol)-*b*-poly(lactic acid) (MPEG-SS-PLA), were prepared to carry paclitaxel (PTX) for glutathione (GSH)-regulated drug delivery. The PTX-loaded MPEG-SS-PLA NPs were fabricated using an optimized oil-in-water emulsion/solvent evaporation method. The size and morphology of the prepared NPs were characterized by scanning electron microscopy (SEM). The SEM results demonstrate that the NPs were dispersed as individual particles and were rice-shaped. The PTX loading efficiency, *in vitro* release, and stability of the NPs were analyzed by high-performance liquid chromatography (HPLC). The HPLC results revealed that the NPs released almost 90% PTX within 96 h when GSH presented at intracellular concentrations, whereas only a very small PTX amount was released at plasma GSH levels. The *in vitro* cytotoxicities of the NPs against A549, MCF-7, and HeLa carcinoma cells were assessed using a standard methyl thiazolyl tetrazolium (MTT) assay. The MTT assay results show that the NPs caused concentration- and time-dependent changes in cell viability. To investigate the cellular uptake of the PTX-loaded NPs, visual endocytosis assay was performed using the fluorescent dye coumarin-6 as a model drug. The endocytosis assay results reveal rapid penetration and intracellular accumulation of coumarin-6-loaded NPs, as well as rapid coumarin-6 dispersion from the NPs. Overall, these findings establish that the NPs containing the synthesized redox-responsive polymer MPEG-SS-PLA can be used as potential carrier systems for antitumor drug delivery.

© 2011 Elsevier B.V. All rights reserved.

1. Introduction

Paclitaxel (PTX), isolated from the bark of Pacific Yew (*Taxus brevifolia*; family Taxaceae), is believed to be one of the best antineoplastic drugs discovered from nature. In clinical trials, it has shown significant activity against a wide variety of tumors, including refractory ovarian, metastatic breast, non-small cell lung cancers, and so on [1–3]. PTX functions by promoting the assembly and stabilization of microtubules that interfere with mitotic spindle function, ultimately arresting cells in the G₂/M phase of mitosis [3]. However, the clinical applications of PTX have been hampered by its low aqueous solubility and fast clearance from plasma [4]. The currently available version of PTX is formulated in a vehicle composed of a 50:50 (*v/v*) mixture of Cremophor EL (polyoxyethylated castor oil) and dehydrated alcohol. Cremophor[®] EL has been reported

to cause serious side effects, such as hypersensitivity reactions, nephrotoxicity, neurotoxicity, and cardiotoxicity [4,5]. To date, the extensive clinical use of PTX is somewhat hindered by the lack of appropriate delivery vehicles [5].

To maintain the high activity of PTX against many cancer types and surmount the problems associated with its formulation, new formulations involving micelles, liposomes, and polymeric nanoparticles (NPs) have been developed to improve PTX delivery [6–8]. Among these formulations, polymeric NPs have attracted the greatest interest given their structural and compositional flexibility; such attributes result in enhanced drug solubility, prolonged drug blood circulation time, decreased side effects, and improved drug bioavailability [8–10].

Generally, amphiphilic polymeric NPs self-assemble in aqueous solutions. Hydrophobic drugs can be encapsulated in the hydrophobic NP core, leaving the hydrophilic parts on the NP surface [8,10]. However, drug release from common polymeric NPs is delayed to some degree because of their lack of response to intracellular stimuli. This inefficient drug release from the vehicle into the cytoplasm results in insufficient anticancer drug concentration in cancer sites. Consequently, drug resistance occurs, resulting in the requirement for higher drug dosage and increased systemic

* Corresponding author at: Colleges of Science and Veterinary Medicine, Northwest A&F University, Yangling, Shaanxi 712100, PR China. Tel.: +86 29 87082520; fax: +86 29 87082520.

E-mail address: jywang@nwsuaf.edu.cn (J. Wang).

¹ These authors contributed equally to this work.

side effects [11–13]. For these reasons, the synthesis of intracellular stimuli-responsive and biocompatible polymers (as well as their nanostructure preparation) for anticancer drug delivery has been gaining popularity. Stimuli-responsive nanovehicles are very important especially when the stimuli are unique to the disease pathology. Upon reaching the targeted tumor, they can release the drug as triggered and mediated by intracellular stimuli, which are specific to the pathological “triggers”, such stimuli include pH [14], temperature [15], glutathione (GSH) [16,17], and enzymes [18]. Stimuli-responsive carriers are essential in drug delivery, in which the delivery system induces aggressive activity against tumor cells because optimal therapeutic efficacy with reduced side effects is achieved [12,19].

Among current intracellular stimuli-responsive drug delivery systems, redox-sensitive polymers and their nanodrug carriers have drawn increasing interest because they contain redox-sensitive polymers with a high redox potential difference (~100–1000-fold) between the reducing intracellular space and the oxidizing extracellular space [20].

GSH, a thiol-containing tripeptide, reduces disulfide bonds in the cytoplasm. A previous study has demonstrated that GSH concentration in intracellular spaces (2–10 mmol/L) is substantially higher than that in the cellular exterior (~2 μmol/L) [20]. This dramatic concentration variation makes GSH a potential stimulus for the delivery of some therapeutics. Disulfide linkages are stable in the oxidizing environment of the bloodstream, but are degraded rapidly in the cytosol [21]. This feature of the disulfide bond makes it unique in both biological and bioengineering systems for redox-sensitive controlled release. Drug delivery systems containing disulfide linkages can provide significant efficacy improvement in drug delivery and release [16,22].

In the present study, a new disulfide bond-containing redox-sensitive polymer, poly(ethylene glycol)-*b*-poly(lactic acid) (MPEG-SS-PLA), was synthesized. Its components are poly(ethylene glycol)monomethyl ether (MPEG) and polylactic acid (PLA). These components were introduced into the polymer for three reasons. First, MPEG and PLA are two of the most popular non-cytotoxic and biodegradable polymers approved by the Food and Drug Administration [23]. Second, MPEG is known to impart protein and cellular stealth properties to surfaces and interfaces. MPEG-modified nanostructures can effectively inhibit reticuloendothelial system sequestration, escape rapid uptake by phagocytic cells, and prolong blood circulation time; all these are enabled by MPEG molecules that create a protective layer on the nanostructure surface to inhibit opsonization [24,25]. Finally, PLA is a representative polyester that has been widely used to form the hydrophobic segment and core of polymeric NPs.

Rice-shaped PTX-loaded MPEG-SS-PLA NPs were then prepared using the synthesized MPEG-SS-PLA and an optimized oil-in-water (O/W) emulsion/solvent evaporation method. GSH-regulated PTX release, *in vitro* cytotoxicity, and cellular uptake of these PTX-loaded redox-responsive polymeric NPs were investigated. A human lung adenocarcinoma epithelial cell line (A549 cells), a human breast adenocarcinoma cell line (MCF-7 cells), and a human cervical carcinoma cell line (HeLa cells) were used for the investigations.

2. Materials and methods

2.1. Materials

L-lactide was obtained from the Jinan Daigang Biomaterial Co., Ltd. (Shandong, China) and was recrystallized from anhydrous

ethyl acetate thrice. Bis(2-hydroxyethyl) disulfide (HES; 98%) was purchased from TCI (Shanghai, China). MPEG (number average molecular weight, $M_n = 5000$), D- α -tocopheryl polyethylene glycol 1000 succinate (TPGS), p-nitrophenyl chloroformate (p-NPC; 97%), cystamine dihydrochloride (>98%), 2,2-dithiodipyridine (Py-SS-Py; >98%), and 2-mercaptopyridine (Py-SH, 98%) were supplied by Sigma-Aldrich (St. Louis, Mo, USA). L-GSH (>98%) and dithiothreitol (DTT; >98%) were received from Beijing Solarbio Science and Technology Co., Ltd. (Beijing, China). PTX was purchased from Xi'an Haohuan Biotech. Co., Ltd. (Xi'an, China). Stannous octoate [$\text{Sn}(\text{Oct})_2$] and coumarin-6 were obtained from J&K Chemical Ltd. (Logan, UT). Monomethoxy-poly(ethylene glycol)-*b*-poly(lactide) (MPEG-PLA; $M_n = 10,537$) was synthesized in our laboratory following the method we previously reported [8]. All solvents and other chemicals were purchased from local commercial suppliers and are of analytical reagent grade, unless otherwise stated. Ultrapurified water was supplied by a Milli-Q system (Millipore®).

2.2. MPEG-SS-PLA synthesis

2.2.1. MPEG-SS-Py synthesis

MPEG-SS-Py was synthesized in a four-step reaction procedure [26]. In the first step, a solution of p-NPC (0.807 g, 4.00 mmol) in methylene chloride (DCM; 7.0 mL) was slowly added to a DCM solution (30.0 mL) of MPEG (5.00 g, 1.00 mmol) and pyridine (0.396 g, 5.00 mmol) under a dry nitrogen atmosphere at 0 °C. After 24 h of reaction at room temperature, the resulting polymer MPEG-NPC was precipitated in excess cold diethyl ether and dried *in vacuo*. In the second step, the dried MPEG-NPC (1.394 g, 0.270 mmol) was first dissolved in dimethyl sulfoxide (DMSO, Amresco Inc., USA; 5.0 mL), and was then added dropwise to a DMSO solution (2.0 mL) of cystamine dihydrochloride (0.306 g, 1.36 mmol) with Et_3N (0.284 g, 2.80 mmol). After 24 h of reaction at 25 °C, the resulting MPEG-cystamine conjugate was precipitated in excess cold diethyl ether and dried *in vacuo*. In the third step, the MPEG-cystamine conjugate (1.382 g, 0.268 mmol) was reacted with DTT (0.308 g, 1.99 mmol) in water (10.0 mL) for 48 h. The product was ultrafiltered on a Molecular/Por ultrafiltration flat membrane [molecular weight (M_w) cutoff = 1000 Da; Molecular/Por®, Spectrum Laboratories, Inc.] and freeze dried (VirTis Bench Top 2K Freezedryer, USA) to yield MPEG-SH. Finally, under a nitrogen atmosphere, MPEG-SH (0.611 g, 0.120 mmol), Py-SS-Py (0.053 g, 0.240 mmol), and a catalytic amount of Py-SH (2.90 mg) were dispersed in 20.0 mL of water. The pH of the resulting mixture was adjusted to 1.5 with an HCl solution (37 wt.%). The mixture was then further reacted for 30 h at room temperature, and its pH was readjusted to neutral pH using NaOH solution (1.0 mol/L). MPEG-SS-Py was ultrafiltered on the Molecular/Por ultrafiltration system, and freeze dried for 48 h to obtain white powder. The ^1H NMR (500 MHz; CDCl_3 ; ppm) results were: 7.65, 8.18, 8.26, and 8.77 (4H, m, $-\text{C}_5\text{H}_4\text{N}$); 3.65 [4H, s, $\text{CH}_3\text{O}(\text{CH}_2\text{CH}_2\text{O})_m\text{CH}_2-$]; 3.38 [3H, s, $\text{CH}_3\text{O}(\text{CH}_2\text{CH}_2\text{O})_m\text{CH}_2-$]; and 3.18 (2H, t, $-\text{CH}_2-\text{SS}-$).

2.2.2. PLA-SH synthesis

L-lactide (10.0 g, 69.4 mmol), HES (0.247 g, 1.60 mmol), $\text{Sn}(\text{Oct})_2$ (0.112 g, 0.276 mmol), and toluene (50.0 mL) were mixed in a pre-dried three-necked flask under a nitrogen atmosphere. The reaction time was 30 h at 110 °C. The resulting viscous mixture was dissolved in DCM and was precipitated in excess cold diethyl ether. The precipitated product (PLA-SS-PLA) was collected and dried *in vacuo*. The product was purified by two rounds of reprecipitation with methylene chloride-cold diethyl ether. The ^1H NMR (500 MHz; CDCl_3 ; ppm) results were: 5.17 [1H, q, $-(\text{COCHCH}_3\text{O})_{2n}-$]; 1.57 [3H, d, $-(\text{COCHCH}_3\text{O})_{2n}-$]; and 2.90 (4H, t, $-\text{CH}_2-\text{SS}-\text{CH}_2-$).

PLA-SH was prepared by dissolving the synthesized PLA-SS-PLA (2.88 g, 0.480 mmol) and DTT (0.785 g, 5.10 mmol) in tetrahydrofuran (THF; 25.0 mL) under a nitrogen atmosphere. An anhydrous methanol solution (2.0 mL) of CH_3ONa (0.0120 g, 0.220 mmol) was added with stirring. After 30 h of reaction time at 25 °C, the resulting PLA-SH was precipitated in cold diethyl ether, filtered under a nitrogen atmosphere, and dried *in vacuo*. The ^1H NMR (500 MHz; CDCl_3 ; ppm) results were: 5.17 [1H, q, $-(\text{COCHCH}_3\text{O})_{2n}-$]; 1.57 [3H, d, $-(\text{COCHCH}_3\text{O})_{2n}-$]; and 2.77 (2H, t, $-\text{CH}_2-\text{SH}$).

2.2.3. MPEG-SS-PLA synthesis

Under nitrogen flow, a DCM solution (30.0 mL) of MPEG-SS-Py (1.89 g, 0.360 mmol) was prepared. Acetic acid was added to the solution to adjust its pH to 3.0, followed by addition of PLA-SH (0.880 g, 0.295 mmol) in DCM (1.0 mL), and the reaction time was 48 h at 30 °C. The resulting polymer MPEG-SS-PLA was precipitated in cold diethyl ether, filtered, and dried *in vacuo* for 48 h. The ^1H NMR (500 MHz; CDCl_3 ; ppm) results were: 3.65 [4H, s, $\text{CH}_3\text{O}(\text{CH}_2\text{CH}_2\text{O})_m\text{CH}_2\text{CH}_2-$]; 3.38 [3H, s, $\text{CH}_3\text{O}(\text{CH}_2\text{CH}_2\text{O})_m\text{CH}_2-$]; 2.86 (2H, t, $-\text{SS}-\text{CH}_2-\text{CH}_2-\text{PLA}$); 2.90 (2H, t, $-\text{SS}-\text{CH}_2-\text{CH}_2-\text{NH}-\text{CO}-$); 5.20 [1H, q, $-(\text{COCHCH}_3\text{O})_{2n}-$]; and 1.59 [3H, d, $-(\text{COCHCH}_3\text{O})_{2n}-$].

2.3. Polymer characterization

The synthesized polymers were characterized by using the ^1H NMR spectra and gel permeation chromatography (GPC) (more details please see [supplementary information](#)).

2.4. Preparation of PTX-loaded MPEG-SS-PLA NPs

The PTX-loaded MPEG-SS-PLA NPs were prepared by a nanoprecipitation method using an O/W emulsion/solvent evaporation technique [27]. MPEG-SS-PLA polymer (10 mg) was dissolved in THF (2.5 mL), and PTX was subsequently added at different drug/polymer feed ratios (w/w). The formed solution was added dropwise (1 mL/min) to aqueous TPGS [15 mL, 0.04% (w/v)] with continuous stirring (400 rpm). The emulsion was stirred for 24 h to produce the shearing force necessary for droplet stretching to facilitate solvent evaporation [27]. After solvent removal by 24 h evaporation at room temperature, the NP suspension was centrifuged at 13,500 rpm for 30 min, and washed twice with ultrapurified water to remove excess TPGS. The resulting pellets were resuspended in ultrapurified (5 mL) water. The product was freeze dried for 48 h and stored at -20°C until use.

Fluorescent MPEG-SS-PLA NPs were prepared in the same manner as the above-mentioned procedure, but 0.1% coumarin-6 was incorporated in the initial organic solution instead of PTX. For drug release comparison studies, PTX-loaded MPEG-PLA NPs were prepared in the same way but by dissolving MPEG-PLA (10 mg), instead of MPEG-SS-PLA, in the initial THF solution.

2.5. Characterization of drug-loaded NPs

2.5.1. Morphology and drug loading

The morphology of the prepared NPs was determined by field emission scanning electron microscopy (SEM; JSM-6700F, JEOL, Japan), and the PTX formulated in the NPs was measured using high-performance liquid chromatography (HPLC; Waters 600E, USA) [9]. More details are shown in [supplementary information](#).

2.5.2. PTX-loaded NP stability

The stability of the PTX-loaded NPs was evaluated for a period of 3 months. The prepared NPs were stored at -20°C . At specific time intervals, freshly prepared samples (1.0 mg) and stored samples (1.0 mg) were separately dissolved in phosphate buffered

saline (PBS; 1.0 mL, 0.01 mol/L, pH 7.4). The resulting solutions were centrifuged at 13,500 rpm for 10 min to separate the diffused PTX. The precipitated NPs were then dissolved in 1.0 mL DCM. The solvent was evaporated at room temperature, and then the residues were reconstituted in acetonitrile/water [1.0 mL, 60:40 (v/v)] for HPLC analysis. At least triplicate test runs were conducted.

2.5.3. In vitro drug release

The redox triggered-release of PTX from MPEG-SS-PLA NPs was carried out in centrifuge tubes. For each tube, NPs (1.0 mg) were dissolved in PBS (1.0 mL, 0.01 mol/L, pH 7.4) containing 0.1% (w/v) Tween 80 to acquire sink conditions. To mimic the redox potential difference between the reducing intracellular space and the oxidizing extracellular space, different GSH amounts were added to each of the NP solutions to form 0, 0.002, 2, and 10 mmol/L release media. PTX-loaded MPEG-SS-PLA NPs (1.0 mg) were then dissolved in PBS (1.0 mL, 0.01 mol/L, pH 7.4) containing 0.1% (w/v) Tween 80. PTX release was analyzed for the first 4 h, and then the release medium was changed from pure PBS buffer to PBS buffer containing GSH (10 mmol/L) for further drug release analysis. The redox-insensitive MPEG-PLA NPs were used as controls. All the centrifuge tubes were kept in a shaker incubator (SKY-100B) at 37 °C with a rotation speed of 150 rpm. At predetermined time intervals, the solutions were centrifuged at 13,500 rpm for 10 min to separate the released PTX from the NPs. The precipitated NPs were resuspended in fresh PBS, and then placed back in the shaker bath for continuous measurements. The supernatants were completely removed for PTX concentration analysis. PTX released from the supernatant was extracted by DCM (2.0 mL). The collected DCM layer was evaporated at room temperature, and the dried PTX was dissolved in acetonitrile/water [1.0 mL, 60:40 (v/v)]. The percentage of PTX released into the supernatant was determined by HPLC following the same procedures above. The quantitative PTX assay was based on a linear standard curve obtained at a concentration range of 0.002–0.01 mg/mL [28].

2.6. In vitro cytotoxicity and cell uptake assay of NPs

In vitro NP cytotoxicity was measured using a standard methyl thiazolyl tetrazolium (MTT) assay [8]. The cytotoxicity study encompasses both the antitumor effect of the PTX-loaded NPs and the cellular compatibility of native NP materials. Meanwhile, an *in vitro* cellular uptake test was performed using a common fluorescent probe method [29,30].

2.7. Statistical analyses

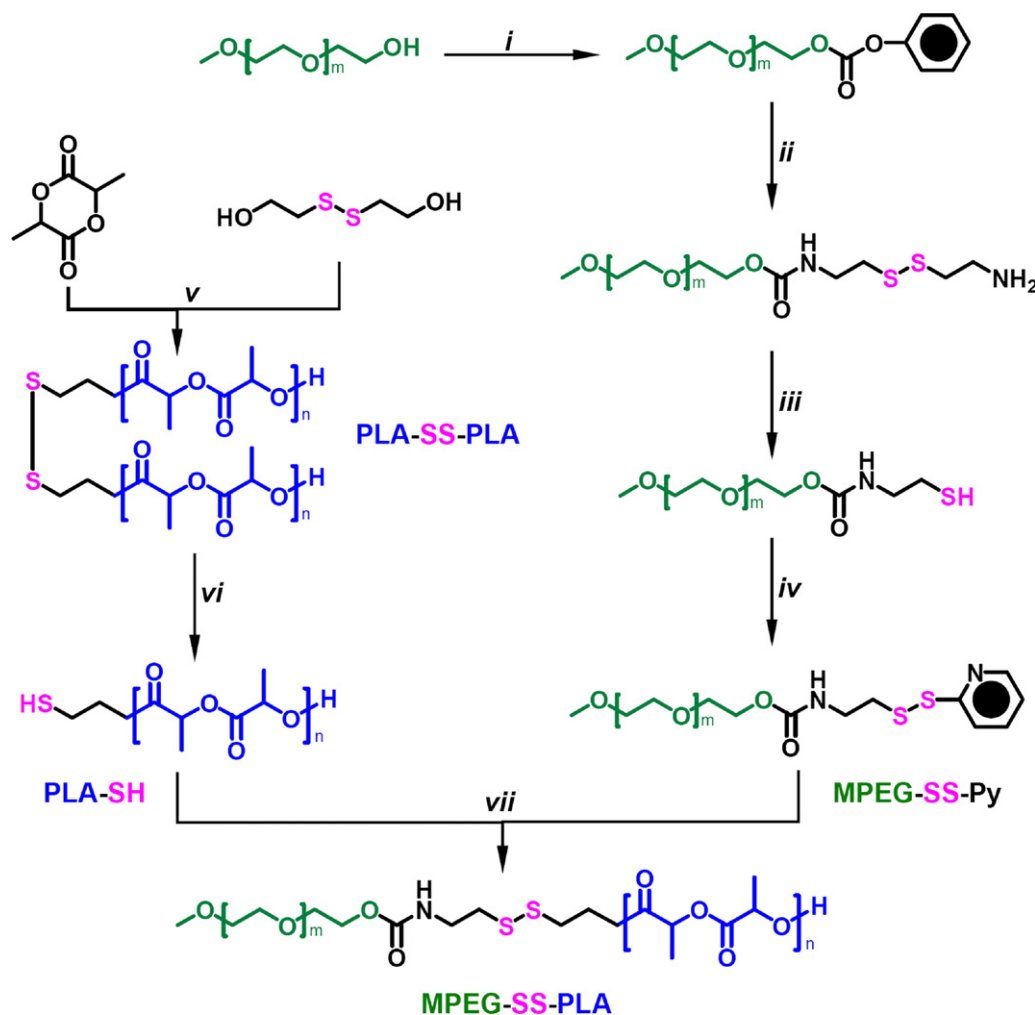
Data for each experiment are expressed as means of three replicates \pm S.D. unless otherwise stated. Mean differences were tested using Duncan's multiple range tests by SPSS 12.0 (SPSS, Inc.). A *p* value of 0.05 was considered statistically significant.

3. Results and discussion

3.1. Polymer synthesis and characterization

The MPEG-SS-PLA polymer with a disulfide linkage between the MPEG and PLA units was synthesized in a seven-step reaction procedure (Scheme 1).

Initially, the MPEG unit (MPEG-SS-Py) was synthesized by (i) activating MPEG-OH with p-NPC [31], (ii) reacting with cystamine dihydrochloride [32], (iii) reducing with DTT to yield MPEG-SH [33], and (iv) activating the thiol group with Py-SS-Py in the presence of a catalytic amount of Py-SH [34]. The ^1H NMR spectrum of MPEG-SS-Py ([supplementary Fig. S1](#)) shows the presence of characteristic



Scheme 1. Synthesis route of MPEG-SS-PLA polymers: (i) p-NPC, pyridine, DCM, 25 °C, 24 h; (ii) cystamine dihydrochloride, Et₃N, DMSO, 25 °C, 24 h; (iii) DTT, H₂O, 25 °C, 48 h; (iv) Py-SS-Py, H₂O, pH 1.5, 30 °C, 30 h; (v) Sn(Oct)₂, toluene, 110 °C, 30 h; (vi) DTT, CH₃ONa, THF, 25 °C, 30 h; (vii) DCM, pH 3.0, 30 °C, 48 h.

peaks assignable to both MPEG and the pyridyl group. Peaks at 3.65 and 3.38 ppm belong to the methylene and methoxyl groups of MPEG. Peaks at 3.18 ppm are assigned to the methylene group of the disulfide linkage. The resonances at 7.65, 8.18, 8.26, and 8.77 ppm assigned to the protons of the pyridyl end group were also observed. The results confirm the successful synthesis of MPEG-SS-Py with an orthopyridyl disulfide functional group.

The preparation of the PLA unit PLA-SH begins from the synthesis of PLA-SS-PLA by the ring-opening polymerization (v) of L-lactide in the presence of the initiator HES and the catalyst Sn(Oct)₂. The structure of the synthesized PLA-SS-PLA was determined by ¹H NMR (supplementary Fig. S2). The peaks at 5.17 and 1.57 ppm belong to a methine (–CH) and a methyl proton (–CH₃)

of the PLA segment, respectively. From the ratio of the peak area at 5.17 ppm to that at 2.9 ppm, the Mn of PLA-SS-PLA was determined to be 6020, which is lower than that determined by GPC (Table 1). This discrepancy may be attributed to the difference in the hydrodynamic properties of the polymers and the polyethylene glycol standards [8]. PLA-SH was then reduced (vi) from PLA-SS-PLA using DTT as a reducing agent and sodium methoxide as a catalyst. The ¹H NMR spectrum of PLA-SH (supplementary Fig. S3) indicates that proton signals at 2.9 ppm from methylene protons adjacent to the disulfide bond (–CH₂–SS–CH₂–) of PLA-SS-PLA was no longer present, and that the characteristic methylene protons next to the thiol end group (–CH₂–SH) peaks at 2.77 ppm appeared. From the integration ratio of the peaks at

Table 1
Molecular weight and molecular weight distribution of polymers.

Polymer	Mn ^a (theoretical)	Mn (¹ H NMR)	Mn (GPC ^b)	Mw ^c (GPC)	Polydispersity index (Mw/Mn)
PLA-SS-PLA	3000–3000	6020	9885	10,319	1.03
PLA-SH	3000	4300	7213	9688	1.34
MPEG-SS-PLA	5000–3000	7700	12,892	14,596	1.13

^a Mn means number average molecular weight.

^b GPC means gel permeation chromatography.

^c Mw means molecular weight.

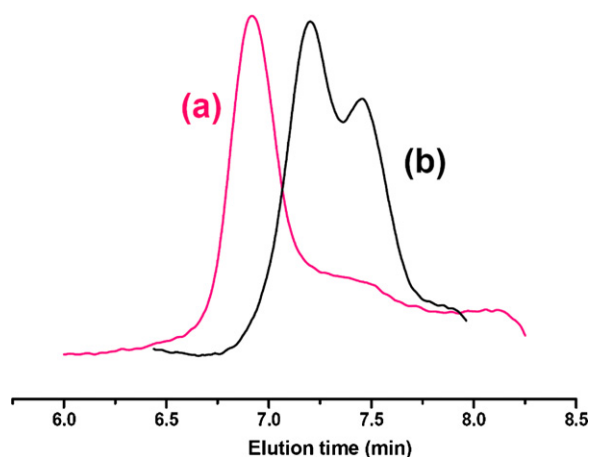


Fig. 1. GPC analysis of the synthesized polymer MPEG-SS-PLA before (a) and after (b) reduction with 10 mmol/L GSH for 2 h.

5.17 ppm to that at 2.77 ppm, the M_n was determined to be 4300, which is almost half of the M_n of PLA-SS-PLA. These support the successful cleavage of the disulfide bonds to yield PLA-SH. GPC analysis shows that the M_n of PLA-SH was 7213 (Table 1). The slightly higher M_w of PLA-SH compared with half of the PLA-SS-PLA is probably due to the loss of low- M_w fractions during precipitation.

Finally, the desired polymer MPEG-SS-PLA was synthesized by the coupling reaction (vii) of PLA-SH and MPEG-SS-Py at a molar ratio of 1:1.2. The ^1H NMR spectrum of MPEG-SS-PLA (supplementary Fig. S4) shows the complete disappearance of pyridyl group resonances at 7.65, 8.18, 8.26, and 8.77 ppm. Peaks assignable to both MPEG (3.65 ppm) and PLA (5.17 and 1.57 ppm) appeared, indicating that the target polymer MPEG-SS-PLA was successfully synthesized by the coupling of MPEG and PLA segments via a disulfide linkage. Compared with the precursor polymers, the average M_w of MPEG-SS-PLA was significantly higher (Table 1), also confirming the successful preparation of MPEG-SS-PLA. Furthermore, the GPC chromatograms (Table 1) show low polydispersity indices, suggesting that the polymers contain a particular chain length with low variability.

To ensure that the synthesized redox-responsive polymer MPEG-SS-PLA is reducible with a reducing agent, GSH was used following a previously reported method [16]. GPC was used to analyze the structural changes in MPEG-SS-PLA before and after the addition of the reducing agent GSH. The results (Fig. 1) show an obvious shift in elution time toward a lower M_n soon after GSH addition, and two peaks appeared. Their average M_n values (5069 and 7174) were close to those of the two functional units MPEG-SH ($M_n = 5103$) and PLA-SH ($M_n = 7213$). This result is within our expectations and is consistent with those of previous studies [35,36], indicating that the synthesized MPEG-SS-PLA can be utilized for drug delivery as a redox-responsive material.

3.2. Preparation of PTX-loaded NPs and PTX loading level assay

Generally, PTX-loaded polymeric NPs are fabricated using O/W emulsion/solvent evaporation [27]. With this technique, prepared polymers can be converted into NPs by dissolving the polymer in a water-miscible organic solvent, and adding this solution to water containing a suitable surfactant. In such a process, the particle morphology and size can be controlled by some key parameters that include the solvent, polymer concentration, ratio of the solvent volume to the water phase volume, and stirring speed [37,38]. Based on numerous optimization studies, we found that MPEG-SS-PLA NP formation most optimally occurred under the following param-

eters: a THF phase containing 4.0 mg/mL polymer, aqueous solution containing 0.04% (w/v) TPGS, a 1:6 volume ratio of THF phase to aqueous phase, and a slow addition rate (1 mL/min) under a stirring speed of 400 rpm. Otherwise, the products were irregularly shaped particles or amorphous aggregates.

Under the optimized conditions and using MPEG-SS-PLA, a series of PTX-loaded NPs with individual and rice shapes was prepared (Fig. 2) in the presence of varying weight percentages of PTX. PTX loading efficiency (LE) and encapsulation efficiency (EE) were analyzed by HPLC. Table 2 summarizes the PTX LE and EE, as well as the size of each NP type. These results demonstrate that the prepared PTX-loaded polymeric NPs possess a high PTX EE (80–90%). The results did not differ significantly among each other.

3.3. Size and stability of drug-loaded NPs

Table 2 shows that when the feed ratio (PTX/polymer, wt.%) was increased from 1% to 3%, no significant effect on the particle size was observed. The average minor axis lengths were consistent at around 130 nm, and the major axis lengths slightly increased from 373.9 ± 4.8 to 426.3 ± 4.1 nm. However, NP particle sizes prepared at feed ratios (PTX/polymer, wt.%) of 5% and 10% were notably larger. The mean particle major axis lengths were 1169.1 ± 9.9 and 2217.4 ± 43.9 nm, and the minor axis lengths were 145.4 ± 3.7 and 159.6 ± 2.0 nm, respectively. This indicates that particle size can be affected by the drug amount when other parameters are kept constant. NP size is directly dependent on the diffusion rate of the organic phase to the aqueous environment. The slower the diffusion rate, the larger the resulting particles. Increased organic phase viscosity can hinder solvent diffusion, thereby producing large particles [11]. In the present work, increased drug amounts in the solvent resulted in higher viscosity, which led to larger particle sizes. Particle size is an important physical property that directly affects cellular uptake capabilities, and ultimately, biodistribution. According to a previous report [39], large particles ($>5 \mu\text{m}$) can be taken up via the lymphatic system and small particles (<500 nm) can cross epithelial cell membranes through endocytosis. Therefore, to obtain a small particle size as well as relatively high drug LE and EE, the PTX-loaded polymeric NPs prepared at a drug/polymer ratio of 3% were selected for further investigation.

The stability assay of the PTX-loaded NPs after one- and three-month storage times showed no noticeable changes in their morphologies and sizes. No significant leakage was detected as well (supplementary Fig. S5). The results confirm that the prepared PTX-loaded MPEG-SS-PLA NPs have long-term stability, which should also facilitate future investigations.

3.4. In vitro drug release

The redox-mediated drug release studies of the prepared PTX-loaded MPEG-SS-PLA NPs were conducted using GSH at an intracellular-reducing GSH level.

Fig. 3 shows the accumulative release curve of PTX from the NPs at different GSH concentrations. At the extracellular GSH level (0.002 mmol/L), the PTX release pattern is similar to that in the release media without GSH. The PTX release from NPs was only 40% within 96 h in the absence of GSH. However, when the GSH concentration increased to the cytosol level (2–10 mmol/L), PTX release was gradually facilitated (Fig. 3A). In the presence of 10 mmol/L GSH (corresponding to an intracellular level), PTX release from the NPs was much faster, reaching almost 90%. These results show that at an intracellular GSH level, the cleavage of disulfide linkages is more pronounced in accelerating the release of PTX. To further demonstrate that the facilitated PTX release from the MPEG-SS-PLA NPs can be ascribed to the stimulus of GSH, the reduction-insensitive MPEG-PLA NPs were used as con-

Table 2
Drug loading efficiency, drug encapsulation efficiency, and mean size of different PTX-loaded polymeric NPs.

Nanoparticles (NPs)	Feed ratio (PTX/polymer) (wt.%)	Drug loading efficiency (LE, wt.%) ^a	Drug encapsulation efficiency (EE, wt.%) ^b	Average major axes (nm)	Average minor axes (nm)
MPEG-SS-PLA NPs	1	0.89	89.00	373.9 ± 4.8	129.5 ± 3.8
	3	2.73	88.67	426.3 ± 4.1	133.5 ± 4.8
	5	4.39	84.14	1169.1 ± 9.9	145.4 ± 3.7
	10	9.07	83.23	2217.4 ± 43.9	159.6 ± 2.0
MPEG-PLA NPs ^c	3	2.58	84.07	437.6 ± 4.9	131.17 ± 5.1

^a LE (wt.%) = (mass of loaded drug/mass of polymer) × 100%.

^b EE (wt.%) = (mass of loaded drug/mass of the initial drug in feed) × 100%.

^c PTX-loaded MPEG-PLA NPs were prepared as controls.

trols (Fig. 3B). PTX release from MPEG-SS-PLA and MPEG-PLA NPs is notably similar to that of the release media without GSH in the first 4 h. However, PTX release became dramatically faster after the addition of 10 mmol/L GSH to the release media. By contrast, PTX release was not influenced (minimal drug release <30%) within 24 h in the reduction-insensitive MPEG-PLA NPs under the same conditions (Fig. 3B). Consistent with our supposition, these results demonstrate that PTX is released from the reduction sensitive MPEG-SS-PLA NPs upon specific activation by the simulated reductive environment of the cellular cytoplasm.

3.5. In vitro cytotoxicity

The efficiency of the PTX-free MPEG-SS-PLA NPs, pure PTX, and PTX-loaded MPEG-SS-PLA NPs on the viability of tumor cells was assessed using standard MTT assays. The concentrations of PTX (0.025–25 μg/mL) used corresponded to drug plasma levels in humans, and were based on clinical drug dosages [29,30]. Meanwhile, the concentrations of the PTX-free NPs (0.001, 0.01, 0.1, 0.5, and 1 mg/mL) corresponded to that of PTX-loaded MPEG-SS-PLA NPs (25 μg/mL PTX in 1 mg/mL NPs). The three tumor cell types (A549, MCF-7, and HeLa) were chosen for the treatment

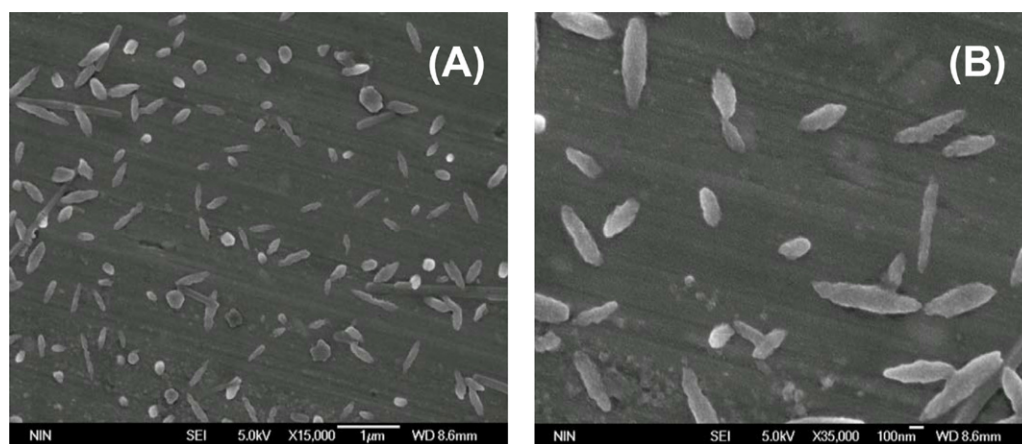


Fig. 2. One set of SEM images of PTX-loaded MPEG-SS-PLA NPs at different magnifications. (A) 15,000× magnification; (B) 35,000× magnification. The PTX-loaded NPs were prepared with 3% feed ratio (PTX/polymer, wt.%), 0.04% (w/v) TPGS, and 400 rpm stirring rate.

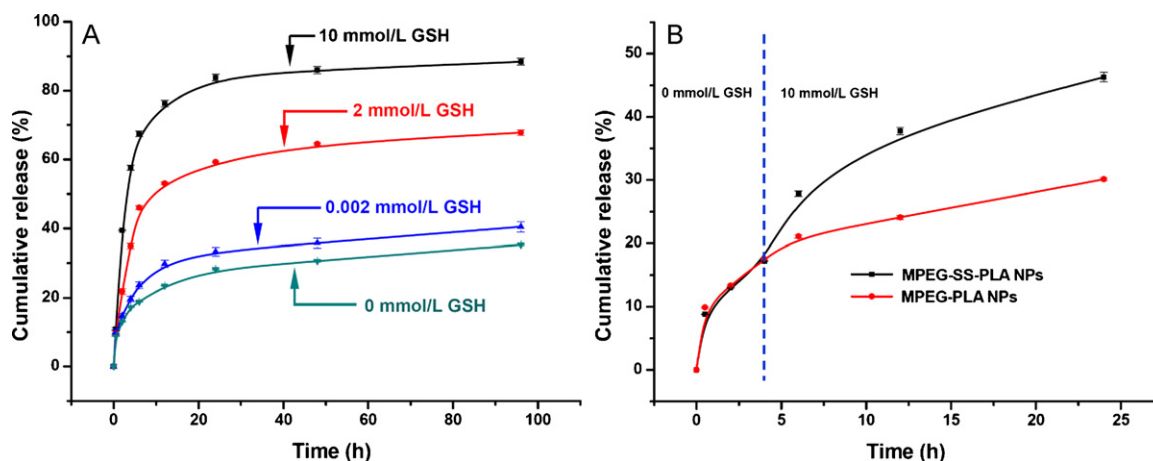


Fig. 3. GSH-mediated drug release. (A) PTX release from PTX-loaded MPEG-SS-PLA NPs in medium comprising 10, 2, 0.002, and 0 mmol/L GSH. (B) PTX release from PTX-loaded MPEG-SS-PLA NPs and PTX-loaded MPEG-PLA NPs by adding GSH (10 mmol/L) at a specific release time (4 h). Each point represents the mean value of n experiments ± S.D. ($n=3$).

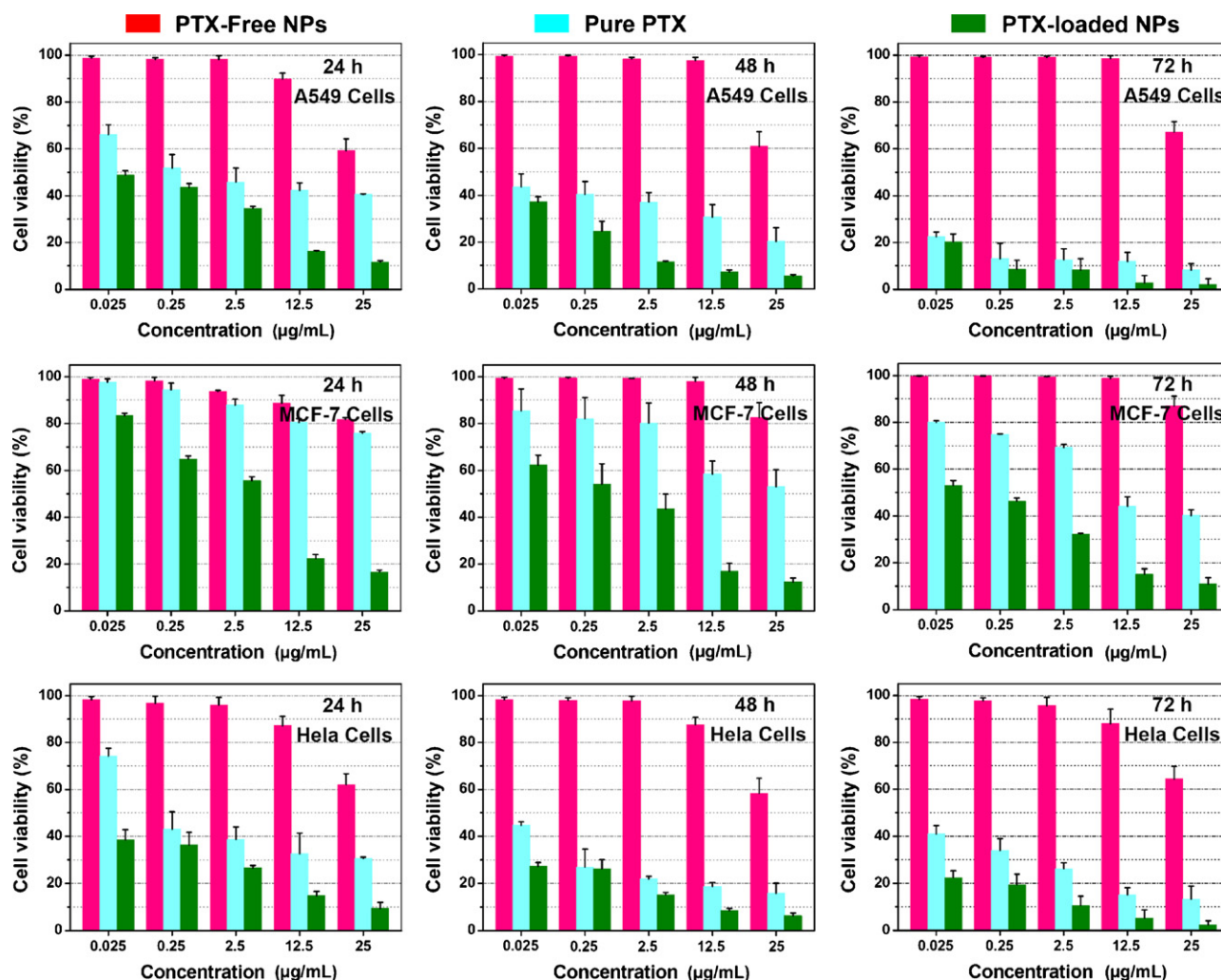


Fig. 4. Cell viabilities of A549, MCF-7, and HeLa cells after 24, 48, and 72 h of treatment with PTX-free MPEG-SS-PLA NPs, pure PTX, and PTX-loaded MPEG-SS-PLA NPs at five PTX concentrations (0.025, 0.25, 2.5, 5, and 25 $\mu\text{g/mL}$) at 37 °C. Given the PTX content in PTX-loaded MPEG-SS-PLA NPs (25 $\mu\text{g/mL}$ PTX in 1 mg/mL NPs), the concentrations of PTX-free MPEG-SS-PLA NPs used here are 0.001, 0.01, 0.1, 0.5, and 1 mg/mL .

experiments based on the clinical oncology application of PTX.

First, the cellular compatibility of PTX-free MPEG-SS-PLA NPs was investigated. The results show that PTX-free NPs at 0.1 mg/mL had nearly no cell injury (Fig. 4). The viabilities of the three cell types were all greater than 95% after 72 h of treatment. No cytotoxic activity was observed in 0.5 mg/mL NPs with A549 and MCF-7 cell treatments for 72 h. However, an overall decline of cell viability occurred at a concentration of PTX-free NPs of up to 1 mg/mL . After 24 h of treatment, the viabilities of the A549, MCF-7, and HeLa cells were $59.19 \pm 5.15\%$, $81.84 \pm 0.68\%$, and $62.02 \pm 4.65\%$, respectively. Moreover, this disturbance of PTX-free NPs did not exacerbate cell viability, but some viable recovery of cells presented after 72-h treatment. The results suggest that the synthesized NP materials at the tested concentrations are lowly cytotoxic and have high cellular compatibility.

The antitumor potential of PTX-loaded NPs was also evaluated. As the positive control, pure PTX treatment largely decreased the viability of A549 cells to $40.56 \pm 0.24\%$, $20.33 \pm 5.88\%$, and $8.19 \pm 2.75\%$ within 24, 48, and 72 h, respectively, at a concentration of 25 $\mu\text{g/mL}$. Furthermore, the viabilities of the MCF-7 and HeLa cells in the 72 h treatment of PTX decreased to $40.22 \pm 2.49\%$ and $13.29 \pm 5.48\%$, respectively. However, the encapsulated PTX presented better antitumor activity. The viabilities of the

A549 cells after 24 h of PTX-loaded MPEG-SS-PLA NP treatment were $48.77 \pm 1.80\%$ (0.025 $\mu\text{g/mL}$), $43.50 \pm 1.71\%$ (0.25 $\mu\text{g/mL}$), $34.63 \pm 0.72\%$ (2.5 $\mu\text{g/mL}$), $16.30 \pm 0.24\%$ (12.5 $\mu\text{g/mL}$), and $11.68 \pm 0.60\%$ (25 $\mu\text{g/mL}$). A high PTX concentration resulted in high A549 cell mortality, which indicates the lower cell viability and more efficient antitumor ability of PTX-loaded MPEG-SS-PLA NPs. These results suggest that the half maximal inhibitory concentration (IC_{50}) of PTX-loaded MPEG-SS-PLA NPs at 24 h can drop to at least 0.025 $\mu\text{g/mL}$, which indicates higher A549 cell mortality than in native PTX. Conversely, the results reveal the time-dependence of cell viability to PTX-loaded MPEG-SS-PLA NP treatments. The viability of the A549 cells decreased to $5.51 \pm 0.60\%$ and $2.04 \pm 2.49\%$, while the treatment times were up to 48 and 72 h, respectively, at a PTX concentration of 25 $\mu\text{g/mL}$. This tendency is consistent with all five designated concentrations of the PTX-loaded MPEG-SS-PLA NPs. Additionally, the viability responses of the other two cell types are similar to that of the A549 cells when treated with PTX-loaded MPEG-SS-PLA NPs. The results show that the viability of MCF-7 cells decreased from $16.62 \pm 0.85\%$ (25 $\mu\text{g/mL}$, 24 h) to $10.93 \pm 2.76\%$ (25 $\mu\text{g/mL}$, 72 h), and that of HeLa cells decreased from $9.46 \pm 2.54\%$ (25 $\mu\text{g/mL}$, 24 h) to $2.33 \pm 1.78\%$ (25 $\mu\text{g/mL}$, 72 h).

The results of the *in vitro* cytotoxicity experiment suggest that the present nano-encapsulation process enhanced the antitumor

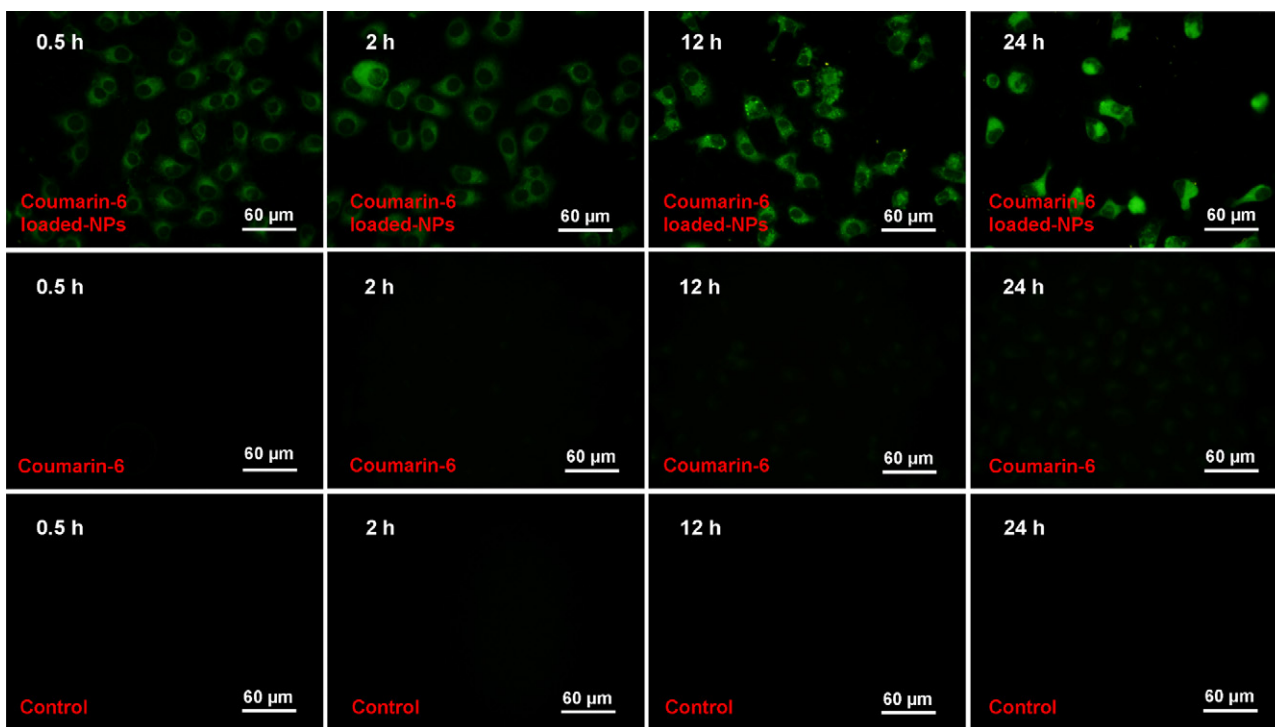


Fig. 5. Cellular uptake of coumarin-6 (5 $\mu\text{g}/\text{mL}$) and coumarin-6-loaded MPEG-SS-PLA NPs (200 $\mu\text{g}/\text{mL}$) in A549 cells.

activity of PTX. PTX-loaded MPEG-SS-PLA NPs led to a lower tumor cell viability *in vitro* compared with pure PTX, consistent with previous reports [29,40]. A possible explanation for this is the intracellular retention and stability of PTX that are very important in tumor cell antiproliferation. The release of PTX from PTX-loaded MPEG-SS-PLA NPs in a triggered and continuous manner resulted in profound cytotoxicity. Additionally, the cellular uptake of the encapsulated PTX can influence the mortality of tumor cells.

3.6. *In vitro* cellular uptake

To investigate the cellular uptake and intracellular distribution of PTX-loaded MPEG-SS-PLA NPs, the green fluorescent dye coumarin-6 was utilized as a model drug. Visual endocytosis assay was performed using coumarin-6-loaded NPs.

Fig. 5 and supplementary Figs. S6 and S7 show that the coumarin-6-loaded NPs penetrated into the cells, and most were distributed around the nucleus. The intracellular fluorescence of all the three tumor cell types became lighter with increased coumarin-6-loaded NP incubation times (0.5, 2, 12, and 24 h). This finding suggests the treatment time-dependent PTX-loaded NP uptakes of A549, MCF-7, and HeLa cells. However, only a small number of fluorescence dots (i.e., coumarin-6-loaded NPs; see supplementary Fig. S8) were observed in the cytoplasm, and a homogeneous fluorescence existed. The most viable explanation for this is that GSH-mediated release resulted in the bond rupture of MPEG-SS-PLA and the fast dispersion of coumarin-6 from the NPs (Fig. 6). This finding demonstrates that the redox triggering of the synthesized NPs has a highly efficient intracellular drug release activity. Meanwhile, the intracellular fluorescence after coumarin-6-loaded NP

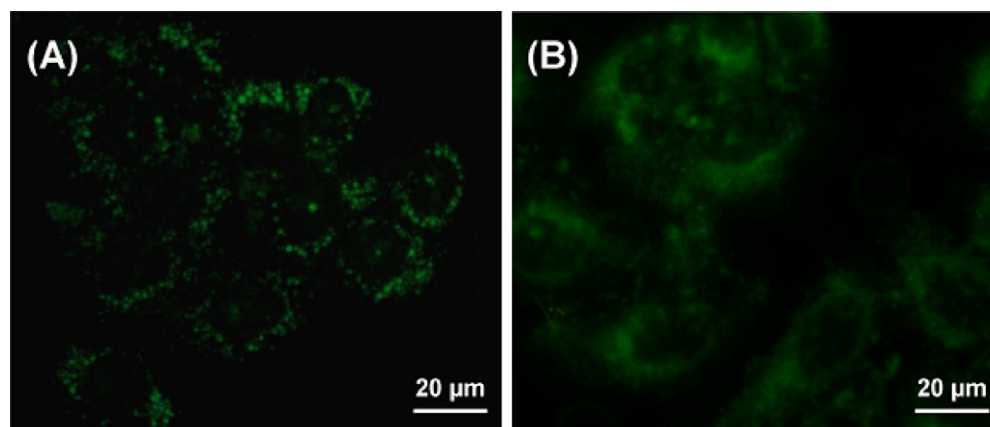


Fig. 6. Cellular uptake of coumarin-6-loaded MPEG-PLA NPs (A) and coumarin-6-loaded MPEG-SS-PLA NPs (B) in HeLa cells. Treatment concentration = 200 $\mu\text{g}/\text{mL}$, incubation time = 0.5 h. Numerous fluorescence dots presented in the cytoplasm after coumarin-6-loaded MPEG-PLA NP treatment. However, mostly homogeneous fluorescence presented in the cytoplasm after coumarin-6-loaded MPEG-SS-PLA NP treatment. This result suggests that redox-triggered MPEG-SS-PLA NPs are able to complete the rapid intracellular dispersion of coumarin-6 from NPs.

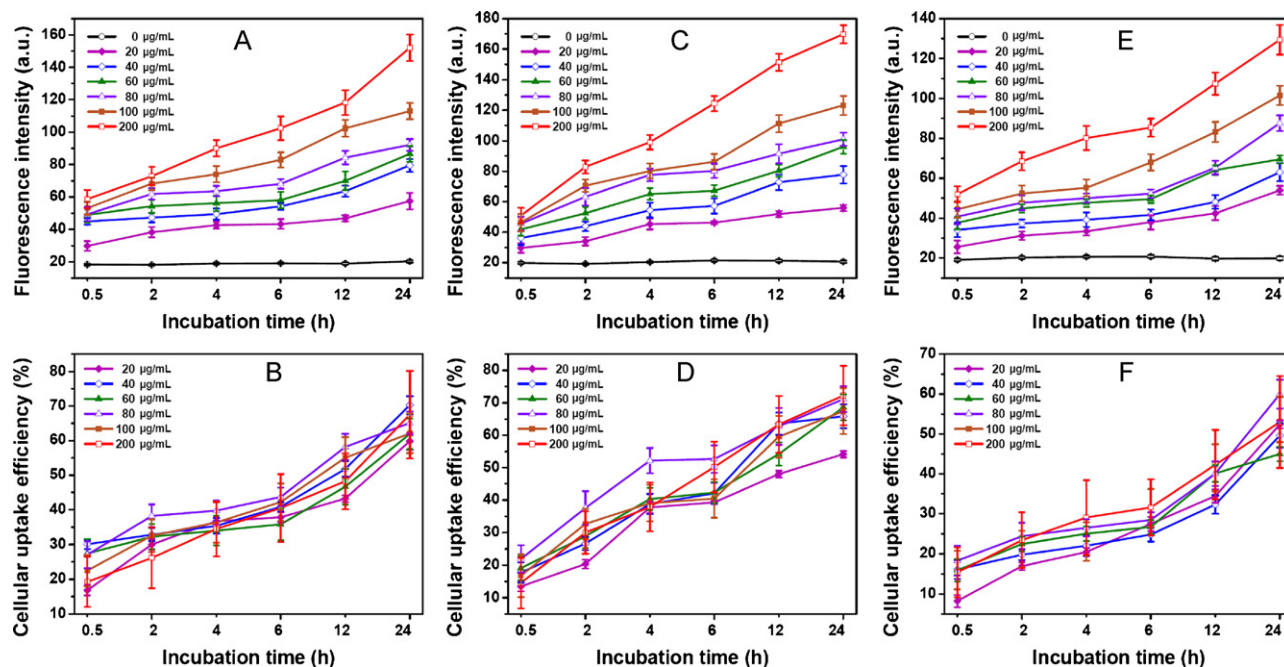


Fig. 7. Cellular uptake analyses of MPEG-SS-PLA NPs in the three types of tumor cells. Up: quantitative fluorescence intensity of cellular uptake in A549 (A), MCF-7 (C), and HeLa (E) cells after incubation of coumarin-6-loaded MPEG-SS-PLA NPs at different concentrations (0, 20, 40, 60, 80, 100, and 200 $\mu\text{g}/\text{mL}$) and different times (0.5, 2, 4, 6, 12, and 24 h). Down: uptake efficiency of A549 (B), MCF-7 (D), and HeLa (F) cells to coumarin-6-loaded MPEG-SS-PLA NPs at concentrations of 20, 40, 60, 80, 100, and 200 $\mu\text{g}/\text{mL}$ at 0.5, 2, 4, 6, 12, and 24 h, respectively.

treatment was largely brighter than that of the coumarin-6 treatment at the same incubation time. These observations suggest that the NPs improved PTX uptake efficiency, which possibly caused the higher cytotoxicity through increased drug concentrations in tumor cells.

A quantitative cellular uptake assay was also performed for further analysis of the degree of endocytosis of the synthesized NPs and for better control of the strategy of using the drug-loaded NPs strategy to defeat tumor cells. For a thorough investigation of cellular uptake, six different concentrations (20, 40, 60, 80, 100, and 200 $\mu\text{g}/\text{mL}$) and six incubating times (0.5, 2, 4, 6, 12, and 24 h) of coumarin-6-loaded NPs were designed based on common research procedures [10,30,40].

Fig. 7 shows that fluorescence intensity increased with both the incubation time and the concentration of coumarin-6-loaded NPs. This result implies the increased accumulation of NPs in all the three tumor cell types. The cellular uptake amount of coumarin-6-loaded NPs at a concentration of 200 $\mu\text{g}/\text{mL}$ was clearly the highest among all concentrations. The cellular uptake efficiency levels of coumarin-6-loaded NPs (200 $\mu\text{g}/\text{mL}$) in A549 cells were $19.29 \pm 7.22\%$ (0.5 h), $26.15 \pm 8.72\%$ (2 h), $34.50 \pm 7.87\%$ (4 h), $40.50 \pm 9.79\%$ (6 h), $48.21 \pm 8.07\%$ (12 h), and $67.52 \pm 12.65\%$ (24 h). However, no significant difference was observed in the cellular uptake efficiency of coumarin-6-loaded NPs among the six concentrations. This phenomenon also presented itself in the MCF-7 and HeLa cells. These results correspond with those of other reports on the cellular uptake activity of drug loaded NPs [10,29]. Higher concentrations and longer treatment times result in higher quantities of accumulated drug-loaded NPs through endocytosis in tumor cells; this brings about more efficient inhibition of tumor cell proliferation and viability [29].

4. Conclusion

A new redox-sensitive polymer (MPEG-SS-PLA) was synthesized, and its PTX-loaded NPs were successfully prepared using

optimized O/W emulsion/solvent evaporation. SEM images show that the prepared PTX-loaded NPs have individual particles and regular rice-like shapes. HPLC analysis reveals that the PTX-loaded polymeric NPs had a high EE and long-term stability (at least 3 months at -20°C). Furthermore, the PTX-loaded polymeric NPs rapidly released PTX under the stimulus of GSH compared with the redox-insensitive MPEG-PLA NPs. *In vitro* cytotoxicity and cellular uptake assays using A549, MCF-7, and HeLa cells demonstrate that the MPEG-SS-PLA NPs had low cytotoxicity, high cytocompatibility, and an ability to assist the endocytotic action of an antitumor drug. All these results indicate that new polymer MPEG-SS-PLA (and its NPs) can be utilized as a new carrier for PTX delivery in tumor therapy. Based on this new redox-sensitive polymer MPEG-SS-PLA, further studies on the introduction of targeting molecules (such as folic acid, monoclonal antibodies, and peptides) and modified NP preparations are currently in progress in our laboratory. *In vitro* and *in vivo* studies of the targeted delivery of antitumor drugs are also our focus.

Acknowledgments

This work was supported by the National Natural Science Foundation of China (Nos. 209 750 82 and 207 750 59), the Ministry of Education of the People's Republic of China (No. NCET-08-0464), and the Northwest A&F University.

Appendix A. Supplementary data

Supplementary data associated with this article can be found, in the online version, at doi:10.1016/j.colsurfb.2011.06.009.

References

- [1] E.M. Wall, M.C. Wan, *Cancer Res.* 55 (1995) 753.
- [2] M.A. Jordan, K. Wendell, S. Gardiner, W. Brent Derry, H. Copp, L. Wilson, *Cancer Res.* 56 (1996) 816.
- [3] C.M. Spencer, D. Faulds, *Drugs* 48 (1994) 784.
- [4] A.K. Singla, A. Garg, D. Aggarwal, *Int. J. Pharm.* 235 (2002) 179.

- [5] H. Gelderblom, J. Verweij, K. Nooter, A. Sparreboom, *Eur. J. Cancer* 37 (2001) 1590.
- [6] S.C. Lee, C. Kim, I.C. Kwon, H. Chung, S.Y. Jeong, *J. Control. Release* 89 (2003) 437.
- [7] J. Wu, Q. Liu, R.J. Lee, *Int. J. Pharm.* 316 (2006) 148.
- [8] J.F. Wang, W.M. Liu, Q. Tu, J.C. Wang, N. Song, Y.R. Zhang, N. Nie, J.Y. Wang, *Biomacromolecules* 12 (2011) 228.
- [9] J. Pan, S.S. Feng, *Biomaterials* 29 (2008) 2663.
- [10] C. Mohanty, S. Sahoo, *Biomaterials* 31 (2010) 6597.
- [11] Y.C. Dong, S.S. Feng, *Biomaterials* 25 (2004) 2843.
- [12] L.Y. Tang, Y.C. Wang, Y. Li, J.C. Du, J. Wang, *Bioconjugate Chem.* 20 (2009) 1095.
- [13] S. Ganta, H. Devalapally, A. Shahiwala, M. Amiji, *J. Control. Release* 126 (2008) 187.
- [14] V. Bulmus, M. Woodward, L. Lin, N. Murthy, P. Stayton, A. Hoffman, *J. Control. Release* 93 (2003) 105.
- [15] C.J. Chun, S.M. Lee, S.Y. Kim, H.K. Yang, S.C. Song, *Biomaterials* 30 (2009) 2349.
- [16] S. Cerritelli, D. Velluto, J.A. Hubbell, *Biomacromolecules* 8 (2007) 1966.
- [17] L.J. van der Aa, P. Vader, G. Storm, R.M. Schiffelers, J.F.J. Engbersen, *J. Control. Release* 150 (2011) 177.
- [18] P.D. Thornton, R.J. Mart, R.V. Ulijn, *Adv. Mater.* 19 (2007) 1252.
- [19] F.H. Meng, Z.Y. Zhong, J. Feijen, *Biomacromolecules* 10 (2009) 197.
- [20] H. Koo, G.W. Jin, H. Kang, Y. Lee, H.Y. Nam, H.S. Jang, J.S. Park, *Int. J. Pharm.* 374 (2009) 58.
- [21] H.P. Yap, A.P.R. Johnston, G.K. Such, Y. Yan, F. Caruso, *Adv. Mater.* 21 (2009) 1.
- [22] G. Saito, J.A. Swanson, K.D. Lee, *Adv. Drug Deliv. Rev.* 55 (2003) 199.
- [23] Y. Li, X.R. Qi, Y. Maitani, T. Nagai, *Nanotechnology* 20 (2009) 055106.
- [24] S.Y. Kim, I.G. Lee, M.Y. Lee, C.S. Cho, Y.K. Sung, *J. Control. Release* 51 (1998) 13.
- [25] Y. Hu, J.W. Xie, Y.W. Tong, C.H. Wang, *J. Control. Release* 118 (2007) 7.
- [26] H.L. Sun, B.N. Guo, R. Cheng, F.H. Meng, H.Y. Liu, Z.Y. Zhong, *Biomaterials* 30 (2009) 6358.
- [27] M.J. Heslinga, E.M. Mastria, O. Eniola-Adefeso, *J. Control. Release* 138 (2009) 235.
- [28] H.F. Liang, C.T. Chen, S.C. Chen, A.R. Kulkarni, Y.L. Chiu, M.C. Chen, H.W. Sung, *Biomaterials* 27 (2006) 2051.
- [29] F. Danhier, N. Lecouturier, B. Vroman, C. Jérôme, J. Marchand-Brynaert, O. Feron, V. Préat, *J. Control. Release* 133 (2009) 11.
- [30] Y. Liu, K. Li, J. Pan, B. Liu, S.S. Feng, *Biomaterials* 31 (2010) 330.
- [31] Z.P. Zhang, S.H. Lee, S.S. Feng, *Biomaterials* 28 (2007) 1889.
- [32] H.S. Yoo, T.G. Park, *J. Control. Release* 70 (2001) 63.
- [33] S. Ghosh, K. Irvin, S. Thayumanavan, *Langmuir* 23 (2007) 7916.
- [34] R.S. Navath, B. Wang, S. Kannan, R. Romero, R.M. Kannan, *J. Control. Release* 142 (2010) 447.
- [35] S. Takae, K. Miyata, M. Oba, T. Ishii, N. Nishiyama, K. Itaka, Y. Yamasaki, H. Koyama, K. Kataoka, *J. Am. Chem. Soc.* 130 (2008) 6001.
- [36] M.Z. Zhang, A. Ishii, N. Nishiyama, S. Matsumoto, T. Ishii, Y. Yamasaki, K. Kataoka, *Adv. Mater.* 21 (2009) 1.
- [37] L. Desbaumes, A. Eisenberg, *Langmuir* 15 (1999) 36.
- [38] J.S. Qian, M. Zhang, L. Manners, M.A. Winnik, *Trends Biotechnol.* 28 (2009) 84.
- [39] Z.P. Zhang, S.S. Feng, *Biomaterials* 27 (2006) 4025.
- [40] U. Westedt, M. Kalinowski, M. Wittmar, T. Merdan, F. Unger, J. Fuchs, S. Schaller, U. Bakowsky, T. Kissel, *J. Control. Release* 119 (2007) 41.